

# Ultrabroadband nonreciprocal transverse energy flow of light in linear passive photonic circuits

Keyu Xia<sup>1,2,3,\*</sup>, M. Alamri<sup>2,\*</sup>, M. Suhail Zubairy<sup>1,\*</sup>

<sup>1</sup>*Institute for Quantum Science and Engineering (IQSE) and Department of Physics and Astronomy, Texas A&M University, College Station, Texas 77843-4242, USA*

<sup>2</sup>*The National Center for Mathematics and Physics, KACST, P.O. Box 6086, Riyadh 11442, Saudi Arabia*

<sup>3</sup>*ARC Centre for Engineered Quantum Systems, Department of Physics and Astronomy, Macquarie University, NSW 2109, Australia*

[keyu@physics.tamu.edu](mailto:keyu@physics.tamu.edu)

**Abstract:** Using a technique, analogous to coherent population trapping in an atomic system, we propose schemes to create transverse light propagation violating left-right symmetry in a photonic circuit consisting of three coupled waveguides. The frequency windows for the symmetry breaking of the left-right energy flow span over 200 nm. Our proposed system only uses linear passive optical materials and is easy to integrate on a chip.

© 2013 Optical Society of America

**OCIS codes:** (230.1150) All-optical devices; (270.1670) Coherent optical effects; (230.7370) Waveguides

---

## References and links

1. J. Fujita, M. Levy, R. Osgood, L. Wilkens, and H. Dotsch, "Waveguide optical isolator based on machzehnder interferometer," *Appl. Phys. Lett.* **76**, 2158–2160 (2000).
2. F. D. M. Haldane and S. Raghu, "Possible realization of directional optical waveguides in photonic crystals with broken time-reversal symmetry," *Phys. Rev. Lett.* **100**, 013904 (2008).
3. Z. Wang and Y. Chong and J. D. Joannopoulos and M. Soljačić, "Observation of unidirectional backscattering-immune topological electromagnetic states," *Nature (London)* **461**, 772–775 (2009).
4. Y. Shoji, M. Ito, Y. Shirato, and T. Mizumoto, "Mzi optical isolator with si-wire waveguides by surface-activated direct bonding," *Opt. Express* **20**, 18440–18448 (2012).
5. Y. Shen, M. Bradford, and J. T. Shen, "Single-photon diode by exploiting the photon polarization in a waveguide," *Phys. Rev. Lett.* **107**, 173902 (2011).
6. L. Bi, J. Hu, P. Jiang, D. H. Kim, G. F. Dionne, L. C. Kimerling, and C. A. Ross, "On-chip optical isolation in monolithically integrated non-reciprocal optical resonators," *Nature Photon.* **5**, 758–762 (2011).
7. L. Fan, J. Wang, L. T. Varghese, H. Shen, B. Niu, Y. Xuan, A. M. Weiner, and M. Qi, "An all-silicon passive optical diode," *Science* **335**, 447–450 (2012).
8. Z. Yu and S. Fan, "Complete optical isolation created by indirect interband photonic transitions," *Nature Photon.* **3**, 91–94 (2009).
9. M. S. Kang, A. Butsch, and P. S. J. Russell, "Reconfigurable light-driven opto-acoustic isolators in photonic crystal fibre," *Nature Photon.* **5**, 549–553 (2011).
10. Q. Wang, F. Xu, Z. Yu, X. Qian, X. Hu, Y. Lu, and H. Wang, "A bidirectional tunable optical diode based on periodically poled linbo3," *Opt. Express* **18**, 7340–7346 (2010).
11. S. Manipatruni, J. T. Robinson, and M. Lipson, "Optical nonreciprocity in optomechanical structures," *Phys. Rev. Lett.* **102**, 213903 (2009).
12. M. Hafezi and P. Rabl, "Optomechanically induced non-reciprocity in microring resonators," *Opt. Express* **20**, 7672–7684 (2012).
13. Y. Hadad and B. Z. Steinberg, "Magnetized spiral chains of plasmonic ellipsoids for one-way optical waveguides," *Phys. Rev. Lett.* **105**, 233904 (2010).

14. A. B. Khanikaev, S. H. Mousavi, G. Shvets, and Y. S. Kivshar, “One-way extraordinary optical transmission and nonreciprocal spoof plasmons,” *Phys. Rev. Lett.* **105**, 126804 (2010).
15. C. Eüter, K. G. Makris, R. El-Ganainy, D. N. Christodoulides, M. Segev, and D. Kip, “Observation of paritytime symmetry in optics,” *Nature Phys.* **6**, 192–195 (2010).
16. A. Guo, G. J. Salamo, D. Duchesne, R. Morandotti, M. Volatier-Ravat, V. Aimez, G. A. Siviloglou, and D. N. Christodoulides, “Observation of pt-symmetry breaking in complex optical potentials,” *Phys. Rev. Lett.* **103**, 093902 (2009).
17. H. Ramezani, T. Kottos, R. El-Ganainy, and D. N. Christodoulides, “Transition from discrete to continuous townes solitons in periodic media,” *Phys. Rev. A* **82**, 043803 (2010).
18. L. Feng, M. Ayache, J. Huang, Y. Xu, M. Lu, Y. Chen, Y. Fainman, and A. Scherer, “Nonreciprocal light propagation in a silicon photonic circuit,” *Science* **333**, 729 (2011).
19. L. Feng, M. Ayache, J. Huang, Y. Xu, M. Lu, Y. Chen, Y. Fainman, and A. Scherer, “Response to comment on “nonreciprocal light propagation in a silicon photonic circuit”,” *Science* **335**, 38–c (2012).
20. S. Fan, R. Baets, A. Petrov, Z. Yu, W. F. J. D. Joannopoulos, A. Melloni, M. Popović, M. Vanwolleghem, D. Jalas, M. Eich, M. Krause, H. Renner, E. Brinkmeyer, and C. R. Doerr, “Comment on “nonreciprocal light propagation in a silicon photonic circuit”,” *Science* **335**, 38–b (2012).
21. C. Wang, C. Zhou, and Z. Li, “On-chip optical diode based on silicon photonic crystal heterojunctions,” *Opt. Express* **19**, 26948–26955 (2011).
22. C. Wang, X. Zhong, and Z. Li, “Linear and passive silicon optical isolator,” *Scientific Rep.* **2**, 1–6 (2012).
23. M. O. Scully and M. S. Zubairy, *Quantum Optics* (Cambridge University Press, United Kingdom, 1997).
24. S. Longhi, “Transfer of light waves in optical waveguides via a continuum,” *Phys. Rev. A* **78**, 013815 (2008).
25. G. Della Valle, M. Ornigotti, T. Fernandez, P. Laporta, S. Longhi, A. Coppa, and V. Foglietti, “Adiabatic light transfer via dressed states in optical waveguide arrays,” *Appl. Phys. Lett.* **92**, 011106 (2008).
26. S. Longhi, “Optical analog of population trapping in the continuum: Classical and quantum interference effects,” *Phys. Rev. A* **79**, 023811 (2009).
27. A. Crespi, S. Longhi, and R. Osellame, “Photonic realization of the quantum rabi model,” *Phys. Rev. Lett.* **108**, 163601 (2012).
28. K. Okamoto, *Fundamentals of Optical Waveguides* (Academic Press, New York, 2000).
29. H. F. Taylor and A. Yariv, *Proc. IEEE* **62**, 1044 (1974).
30. A. Hardy and W. Streifer, “Coupled mode theory of parallel waveguides,” *J. Lightwave Tech.* **3**, 1135–1146 (1985).
31. K. G. Makris, R. El-Ganainy, D. N. Christodoulides, and Z. H. Musslimani, “Beam dynamics in pt symmetric optical lattices,” *Phys. Rev. Lett.* **100**, 103904 (2008).

---

## 1. Introduction

The integration of nonreciprocal photonic devices on Si or CMOS platforms has been challenging in the past decades. The known optical nonreciprocity can be divided into two classes: forward-backward nonrecipricity (FBNR) and left-right nonrecipricity (LRNR). The first class of nonreciprocal component can be realized by various approaches using the magneto-optic effects [1, 2, 3, 4, 5, 6], nonlinearity [7], a modulation media [8, 9, 10], optomechanics [11, 12], or magnetized plasmonic metal [13, 14]. It can be used for optical isolators. To date, the LRNR, indicating the nonreciprocal light flow between left and right ports of photonic circuits, has been discussed in an array of coupled waveguides by only a few research groups [15, 16, 17]. If the complex optical potential causes the parity-time (PT) symmetry breaking, two coupled waveguides can show a LRNR light transfer in the transverse direction [15, 16]. The realization relies on the precise control of the active medium. Although unclear for optical isolators, the photonic circuit with the left-right nonrecipricity may merge the incident light beams.

The need for integration of optical nonreciprocal elements on a Si/CMOS chip platform is a long-standing problem. The realization of the nonreciprocal light propagation in a completely linear optical medium can strongly impact on both fundamental physics, and also vast applications for integrated optics because of the compatibility with the Si material and CMOS chips. Again based on the PT symmetry breaking induced by a periodic modulation of complex optical potential, Feng et al. stated that they, for the first time, observed the nonreciprocal light propagation in a linear passive optical material [18]. Unfortunately, they admitted their mistake [19] after Fan et al. commented on their work [20]. Another experimental realization of on-chip

optical diodes using all-dielectric, passive, and linear silicon photonic crystal structures is reported by Wang et al. [21, 22]. They confidentially explained why it is possible to make optical diodes using a spatial symmetry breaking geometry in a passive and linear optical medium [22].

In the LRNR, the input light is always localized in one waveguide [15, 16, 17]. This is similar to the coherent population trapping in a three-level  $\Lambda$ -type atom [23]. While the bending waveguide array can simulate well the quantum dynamics of atoms. The classical optical analogs of coherent population transfer [24, 25] and population trapping in the continuum [26] and Rabi oscillation [27] as well has been proved by Longhi's group. Although the trapping of equal light in two waveguides has been discussed [24], the results did not show a valid LRNR of light flow. A theory work indicated that the critical large nonlinearity is necessary to induce nonreciprocity [17] in two evanescently coupled waveguides. However the LRNR in the transverse light flow has been recently observed [15, 16]. Moreover, the three/many-body systems behavior essentially different from the simple two-body system studied in [17]. At least, the optical trapping in coupled three waveguides analogous to the atomic CPT can not be achieved in an optical system composing of two waveguides. It is interesting if one can realize the non-reciprocal wave propagation in evanescently coupled linear and passive waveguides. We expect to achieve the LRNR in a waveguide array. This is the motivation of our work.

Here we propose simple methods to generate the second class of optical nonreciprocity in an array of three coupled waveguides only making from linear, passive optical materials. We focus on the nonreciprocal transverse energy flow between left and right optical waveguides. Thanks to a small dispersion of a linear waveguide, our system can behave in a nonreciprocal manner in an ultrabroad band. The results by numerical simulation of beam propagating method (BPM) and solving the coupled mode equation (CME) demonstrate the breaking of symmetry of transverse energy flow.

## 2. Setup and model

Our system, shown in Fig. 1, is composed of three coupled waveguides embedded in a wafer of width  $W$  and length  $L$ . The middle waveguide  $D_3$  couples to the waveguides  $D_1$  and  $D_2$ . We assume that the coupling between the waveguides  $D_1$  and  $D_2$  is negligible. We also assume that the two side waveguides are lossless but some loss can be included in the middle one. In our photonic system, eigenmodes in the individual waveguide exchange energy via their evanescent fields when two waveguides are close. The couplings are denoted as  $\kappa_{13}$  and  $\kappa_{23}$ , and decrease as the distance  $d_{13,23}$  between two waveguides increases. The coupling between  $D_1$  and  $D_2$  is assumed vanishing because these two waveguides are far enough from each other. The field in  $D_3$  decays exponentially with a constant  $\gamma$  that can be controlled [15, 18, 16].

The evolution of power of field in photonic circuits can be studied either by numerical solving the Helmholtz equation or with the derived coupled mode theory. However the later presents a clearer physic understanding. We first present the approach based on Helmholtz equation.

We consider our system to be two-dimensional (2D). This is reasonable if the size of waveguide in the  $y$  direction is much larger than that in the  $x$  direction. The propagation of the field  $E$  in the photonic circuits in a 2D space can be described by the Helmholtz equation, which takes the form

$$\frac{\partial^2 E}{\partial z^2} + \frac{\partial^2 E}{\partial x^2} + k_0^2 \epsilon(x, z) E = 0, \quad (1)$$

where  $z$  is the propagating direction,  $x$  is the transverse direction, and  $k_0 = \frac{2\pi}{\lambda}$  is the wave vector of field with wavelength  $\lambda$  in the free space. The dielectric constant  $\epsilon(x, z)$  plays the role of the optical potential. We can resolve the field  $E$  into its slowly varying amplitude  $\psi$  and a fast oscillating factor,  $E = \psi e^{\pm j\beta z}$ , where the propagation constant  $\beta = k_0 n_{eff}$ .  $n_{eff}$  is the effective index of waveguides. The sign before  $\beta$  indicates the propagating direction: minus (plus) for the

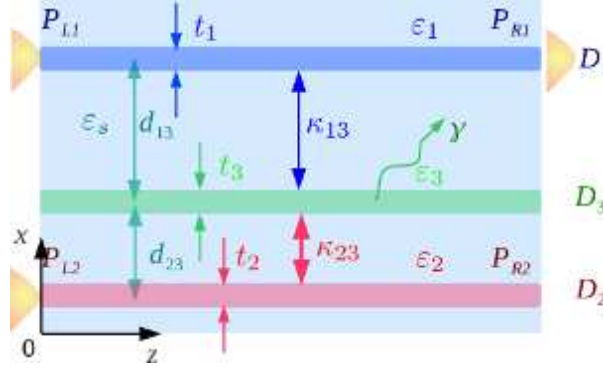


Fig. 1. Light trapping in a photonic circuit consisting of three waveguides embedded in a  $W$  wide,  $L$  long substrate. The coupling  $\kappa_{13} \ll \kappa_{23}$ .  $d_{13,23}$  is the distance between two waveguides. The dielectric constants of substrate is  $\epsilon_s$ , while  $\epsilon_i$  ( $i \in \{1, 2, 3\}$ ) is the constant profile of corresponding individual waveguides  $D_i$  without others. The widths of waveguides are  $t_i$ , respectively.

propagation along the positive (negative)  $z$  direction. In the paraxial approximation  $\left| 2j\beta \frac{\partial \psi}{\partial z} \right| \gg \left| \frac{\partial^2 \psi}{\partial z^2} \right|$ , the amplitude of the field in the photonic circuit evolves according to the equation [28]

$$\mp 2j\beta \frac{\partial \psi}{\partial z} \approx \frac{\partial^2 \psi}{\partial x^2} + k_0^2 [\epsilon(x, z) - n_{eff}^2] \psi. \quad (2)$$

We numerically solve Eq. (2) with BPM to simulate the propagation of field with a spatial resolution  $\delta z = 1 \mu\text{m}$  and  $\delta x = 0.1 \mu\text{m}$ . A finer spatial grid gives the same results. Throughout simulation, we use a Gaussian input profile  $\psi(x, x_0, z = 0, L) = \exp(-(x - x_0)^2 / 2w_p^2)$ , where  $w_p = 1 \mu\text{m}$  is the half width of waist of input field,  $x_0 = x_0^{(i)}$  ( $i \in \{1, 2\}$ ) is the center position of input ports  $P_{L1, L2, R1}$ . The profiles  $\psi(x, x_0^{(1)}, 0)$  and  $\psi(x, x_0^{(1)}, L)$  corresponds to the input field launching into the waveguide  $D_1$  from the port  $P_{L1}$  at  $z = 0$  and  $P_{R1}$  at  $z = L$ , respectively. While the profile  $\psi(x, x_0^{(2)}, 0)$  means an input to the port  $P_{L2}$  at  $z = 0$ . The intensity of the field at the peak is unity. This profile is very close to the fundamental eigenmode of  $D_1$  or  $D_2$ .

Our simulation focuses on a light with wavelength  $\lambda_0 = 1.55 \mu\text{m}$ , which is of interest in optical communications. The photonic circuit can be integrated in a wafer with a substrate dielectric constant  $\epsilon_s = 10.56\epsilon_0$ , where  $\epsilon_0$  is the permittivity of free space. We consider weakly guiding waveguides with  $\epsilon_{core} = 10.76\epsilon_0$  in core. The imaginary part of the dielectric constant in the middle waveguide  $D_3$  is  $\Im\{\epsilon_3\} = -0.01\epsilon_0$ . This induces a loss of  $\gamma = 11.6 \text{ mm}^{-1}$  according to our numerical simulation. The propagation constant is calculated by solving the eigenvalue equation [28] of TE mode. It is evaluated to be  $|\beta| = 1.32593 \times 10^7 \text{ rad/m} \sim k_0(\sqrt{\epsilon_{core}} + \sqrt{\epsilon_s})/2\sqrt{\epsilon_0}$  for all simulation. This is a good approximation for the weakly guiding waveguides.

In our numerical method, the Neumann boundary condition (NBC) is used to greatly suppress the reflection field from the transverse boundary. A small reflection, which can be a practical noise from the boundary of device in experiments, is responsible for the background noise of our numerical results.

Before discussing the results, we present the equivalent, but physically transparent, coupled mode equation approach to explain our system.

The light field  $E$  in photonic circuits can be expressed as a supermode of eigenmodes  $E_i$  of

individual waveguide  $D_i$ , i.e.,

$$E = \sum_{i=1,2,3} A_i E_i = \sum_{i=1,2,3} A_i \psi_i e^{\pm j\beta_i z}, \quad (3)$$

where the amplitude of eigenmode in the  $i$ th waveguide is denoted by  $A_i$  ( $i \in \{1, 2, 3\}$ ). Here  $\psi_i$  is the slowly varying envelope of eigenmode  $E_i$  and  $\beta_i$  is the corresponding propagation constant, which can be controlled by designing the dielectric constant  $\varepsilon_i$  of individual waveguide  $D_i$  and its width  $t_i$ . This parameter also depends on the wavelength of light. According to the coupled mode theory [28, 29, 30] derived from the Helmholtz equation, the dynamics of the modal amplitudes is described by

$$\frac{\partial A_1}{\partial z} = j\Delta_{13}A_1 + j\kappa_{13}(z)A_3 \quad (4a)$$

$$\frac{\partial A_2}{\partial z} = j\Delta_{23}A_1 + j\kappa_{23}(z)A_3 \quad (4b)$$

$$\frac{\partial A_3}{\partial z} = j\kappa_{13}(z)A_1 + j\kappa_{23}(z)A_2 - \gamma A_3, \quad (4c)$$

where  $\Delta_{13} = \beta_1 - \beta_3$  and  $\Delta_{23} = \beta_2 - \beta_3$  are the phase mismatch between waveguides  $D_1$  ( $D_2$ ) and  $D_3$ . The power in the  $i$ th waveguide is evaluated by  $P_i = A_i A_i^*$ . The total power in the system is  $P = \sum_i P_i$ . The phase mismatching and coupling in the coupled mode equation Eq. (4) can be derived from Helmholtz equation Eq. (1). These parameters are dependent on  $k_0$  and the optical potential  $\varepsilon(x, z)$ . The coupling is given by [28, 29, 30]

$$\kappa_{mn} = \frac{k_0^2 \int_s \delta\varepsilon_n E_m^* E_n dS}{\beta_m \int_s E_m^* E_m dS}, \quad (5)$$

where  $s$  denotes the cross section of space and  $\delta\varepsilon_n = \varepsilon(x, z) - \varepsilon_n$  at the cut position  $z$ . For simplicity's sake, we have assumed weakly guiding waveguides and the relation  $\kappa_{mn} = \kappa_{nm}$ . We also neglect the second-order spatial derivatives of the amplitude  $A_i$  and the small self phase shifts due to the perturbation of neighbor waveguides. A full study of the relation of parameter to the Helmholtz equation has been presented by Hardy et al. [29, 30]. Note that the coupled mode theory presents a general model. In contrast, the numerical results depend on the structure of system, and only provides one of many implementations. The different structures can lead to the same set of parameters in the coupled mode equation. On the other hand, the numerical simulation presents a full picture of light in photonic circuits.

Next we turn to our idea about how to create optical nonreciprocity in the transversal energy flow in three coupled waveguides by giving a connection of our classic photonic circuit to a quantum system.

Due to the equivalence between the Helmholtz equation in photonic circuits and the Schrödinger equation in quantum mechanics, the behavior of light propagating in a photonic circuit is similar to the dynamics of the internal atomic states of a quantum system [24, 25]. For example, the normalized light power trapped in optical waveguides plays the role of atomic population. Optical nonreciprocities in an array of coupled waveguides can then be considered as the trapping of input light on demand. As is well known, in a  $\Lambda$ -type three-level atomic systems, we can adiabatically create a target state independent of the initial state of system via the so-called coherent population trapping (CPT) [23]. Our system is analogous to such a  $\Lambda$ -type three-level system. Just as in CPT in the atomic system, we expect to trap most light energy in a selected optical waveguide by suitably controlling the coupling between the waveguides. This

is the basis of the optical nonreciprocity studied in this paper. Note that the LRNR we propose here is substantially different from the FBNR used for optical isolator on the basis of the breaking of Lorentz reciprocity theorem. In the former case, both two sources input into ports in the left hand side but their responses coming out from the right hand side are compared, while the source and the response must exchange in the later. Thus the implementation of the LRNR in a linear, passive medium is not forbidden by the Lorentz reciprocity theorem, which requires the exchange of the place of source and response.

The structure of photonic circuit to create the nonreciprocal transverse energy flow of light is shown in Fig. 2 (a). Through our system, we assume no loss in waveguide  $D_1$  and  $D_2$ . The dielectric constant is  $\epsilon_s = 10.56\epsilon_0$  in the substrate, while it is  $\epsilon_{\text{core}} = 10.76\epsilon_0$  in core of  $w_1$  and  $w_2$ . In waveguide  $w_3$ , the dielectric constant in core is  $\epsilon_3 = (10.76 - 0.01i)\epsilon_0$ . The straight waveguide  $w_3$  is  $4 \mu\text{m}$  wide around its center  $w_3(0) = 26.7 \mu\text{m}$ . The waveguides  $w_1$  and  $w_2$  with width  $2 \mu\text{m}$  are curves along their varying central positions, which are defined as

$$w_1(z) [\mu\text{m}] = \begin{cases} 31; & z < 1.1 \text{ mm} \\ 31 + 3(1 + \sin(2\pi(z - 1350)/1000))/2.0; & z \geq 1.1 \text{ mm} \& z < 1.6 \text{ mm} , \\ 34; & z > 1.6 \text{ mm} \end{cases}$$

and

$$w_2(z) [\mu\text{m}] = \begin{cases} 22; & z < 0.1 \text{ mm} \\ 22 + 1.4(1 + \sin(2\pi(z - 600)/2000))/2.0; & z \geq 0.1 \text{ mm} \& z < 1.1 \text{ mm} \\ 23.4; & z > 1.1 \text{ mm} \end{cases}$$

To fit the numerical results, the coupling  $\kappa_{13}$  and  $\kappa_{23}$  are assumed to vary corresponding to the central positions  $w_1(z)$ ,  $w_2(z)$  and  $w_3(z)$  of waveguides. The other parameters for coupled mode equation are given by:

$$\gamma = 10 \text{ mm}^{-1}, \quad (6)$$

$$\Delta_{13} = \Delta_{23} = 20 \text{ mm}^{-1}. \quad (7)$$

To simulate the varying gaps between waveguides, we assume two gradiently changing coupling strength  $\kappa_{13}$  and  $\kappa_{23}$  as

$$\kappa_{13}(z) [\text{mm}^{-1}] = \begin{cases} 25; & z < 1.1 \text{ mm} \\ 1 + 24(1 - \sin(2\pi(z - 1350)/1000))/2.0; & z \geq 1.1 \text{ mm} \& z < 1.6 \text{ mm} , \\ 1; & z > 1.6 \text{ mm} \end{cases}$$

and

$$\kappa_{23}(z) [\text{mm}^{-1}] = \begin{cases} 2; & z < 0.1 \text{ mm} \\ 2 + 88(1 + \sin(2\pi(z - 600)/2000))/2.0; & z \geq 0.1 \text{ mm} \& z < 1.1 \text{ mm} . \\ 90; & z > 1.1 \text{ mm} \end{cases}$$

The corresponding coupling strength in the propagating direction for Eq. 4 are shown in Fig. 2 (b). Two waveguides in the same chip always couples to each other even if the coupling strength is very small. To consider this coupling, we assume small values as the distance between two waveguides are large. The intensity in waveguides given by the coupled mode equations change very slightly if we neglect this small coupling. We note that, in the absence of loss in the



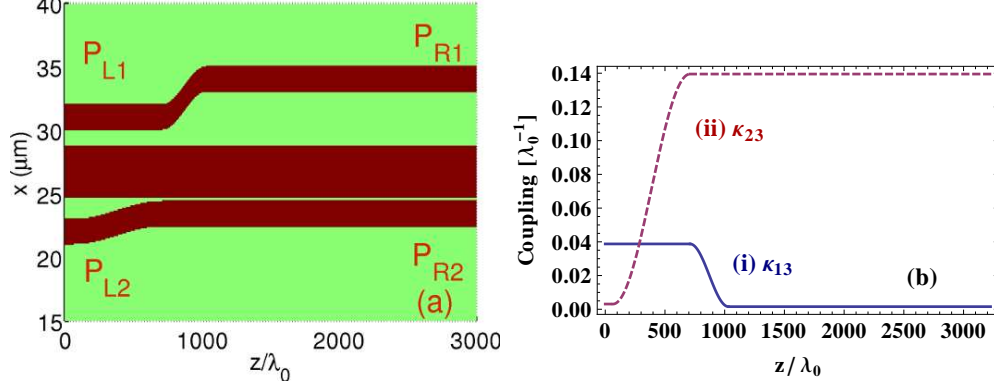


Fig. 2. (a) The waveguide structure for left-right nonreciprocity. (b) The coupling as a function of propagating distance  $z$ . Blue solid lines (i) for  $\kappa_{13}$ , red dashed lines (ii) for  $\kappa_{23}$ . Here  $\lambda_0 = 1.55 \mu\text{m}$ .

waveguide  $w_3$ , the system is reciprocal (not shown here). However if we include loss in the middle waveguide, we create left-right nonreciprocities.

Let us assume that a light with unit amplitude is incident on the port  $P_{L1}$  or  $P_{L2}$  at  $z = 0$ . If the photonic circuit is reciprocal, the transmission from port  $P_{R1}$  or  $P_{R2}$  exchanges as well if the incident exchange. However, in the case of left-right nonreciprocity, the light launched into port  $P_{L1}$  and  $P_{L2}$  always effectively transfer to the waveguide  $D_1$  and comes out from port  $P_{R1}$ . If we use constant couplings  $\kappa_{13}$  and  $\kappa_{23}$ , the LRNR is obtained but the transmissions are small. The energy trapped in waveguide  $D_1$  also decays because part of the energy couples to the middle waveguide from which the energy is lost into the environment at a rate  $\gamma$ . To avoid a strong coupling of energy between  $D_1$  and  $D_3$ , we gradually change the distance between the two side waveguides and the middle one to guarantee an adiabatic process. In addition, large phase mismatches  $\Delta_{13}$  and  $\Delta_{23}$  are used to suppress the energy coupling to waveguide  $D_3$ . In the output side, we decouple the waveguides  $D_1$  and  $D_3$  by introducing a large distance to keep the light energy in  $D_1$  almost constant. The profile of the mode is also kept stable. The couplings used in coupled mode equation for fitting the following numerical results are shown in Fig. 2 (b). These coupling are strongly dependent on the distance  $d_{13,23}$ .

### 3. Results

Now we study the left-right nonreciprocity where we have nonreciprocal light transfer in the transverse direction [15, 31]. Similar to coherent population trapping in quantum optics, we can trap most light energy in the selected waveguide  $D_1$  by designing a weak coupling  $\kappa_{13}$  in comparison with  $\kappa_{23}$ . Our numerical results shown in Figs. 3 (a) and (c) demonstrate a left-right nonreciprocal transverse energy flow. Whatever port  $P_{L1}$  or  $P_{L2}$  we choose to launch the light into, most of the light is trapped in the waveguide  $D_1$ , and comes out from the same port  $P_{R1}$  (blue lines). The transmission for light input into port  $P_{L2}$  is about 27% (Figs. 3 (b)) but it increases to 40% if the light is incident into port  $P_{L1}$  (Figs. 3 (d)). The light in the waveguide  $D_2$  leaks to  $D_3$  and subsequently is absorbed as it propagates. The contrast ratios of light intensities in waveguides  $D_1$  and  $D_2$  are higher than 29 dB in both cases.

So far we presented results based on the numerical solution of the Helmholtz equation. Next we compare these results with the solution of the coupled mode equation Eq. (4), see dashed lines in Figs. 3 (b) and (d). Clearly, the coupled mode theory agrees well with the numeri-

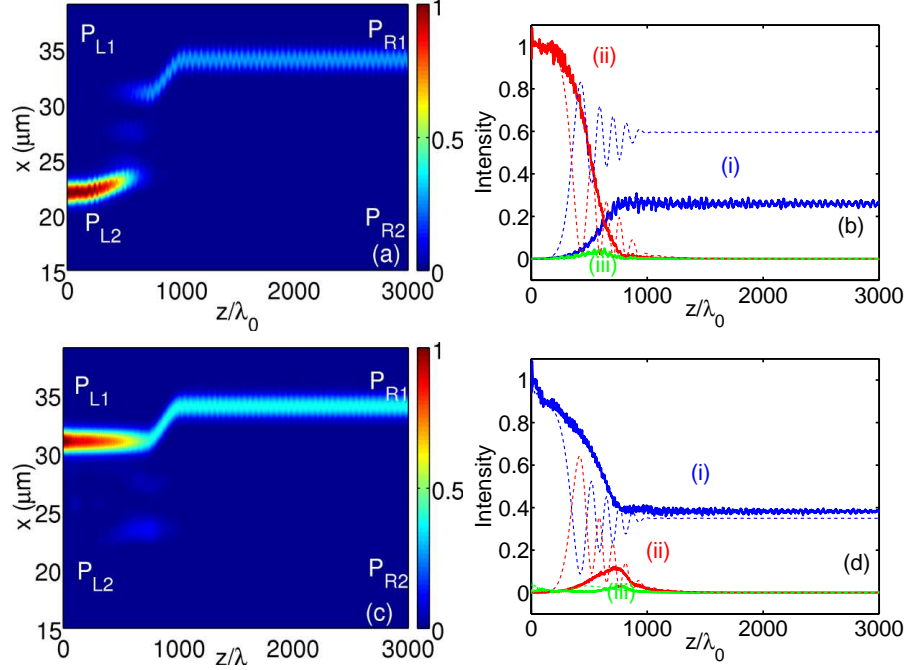


Fig. 3. Left-right nonreciprocity corresponding to Fig. 2 (b). The field propagates from left to right in photonic circuits. (a) Light incident into the waveguide  $D_2$ ; (c) light enters the waveguide  $D_1$ ; (b) and (d) Intensities of field at the middle of waveguides  $D_1$  [blue lines (i)],  $D_2$  [red lines (ii)] and  $D_3$  [green lines (iii)]. Dashed thin lines are the corresponding plots by solving Eq. (4).

cal simulation. However, the coupled mode equations predict power oscillations in the coupled regions. Moreover, the intensity of light in waveguide  $D_1$  in Figs. 3 (b) are higher than the numerical results of BPM method. The origin of discrepancy are complex. In our numerical simulation, the waveguide is  $2\ \mu\text{m}$  or  $4\ \mu\text{m}$  wide, and enough to support higher modes. The width of waveguides  $D_{1,2}$  also change slightly in the bending region. In this region, the fundamental mode couples to higher modes and lose to environment. There are also many controlling parameters in the coupled mode equation Eq. (4). We do not know the exact varying values of these parameters corresponding to the structure of system. In addition, we use a simple model, Eq. (4), in which the parameters are different from the values given by a full coupled mode theory [29, 30]. Thus it is difficult to perfectly fit the numerical results with the coupled mode theory. In spite of small discrepancy, the coupled mode theory still fits numerical results in principle.

The bandwidth in which the propagating light show nonreciprocal behavior is an important feature. We study the frequency dependence of the transmission spectra in Fig. 4 by numerical simulations. As the widths and refractive indices of the two side waveguides  $D_1$  and  $D_2$  are the same, the propagating constants  $\beta_1$  and  $\beta_2$  are equal. Thus the phase mismatch  $\Delta_{13}$  is equal to  $\Delta_{23}$  ideally. As a result, the transmissions are insensitive to the frequency of incident light. Thus our system has an ultrabroadband nonreciprocal window over  $200\ \text{nm}$ , from  $1.6\ \mu\text{m}$  to  $1.8\ \mu\text{m}$ . According to Eqs. (1) and (2), the structure of system is scalable in size to shift this frequency window. In the nonreciprocal windows, the light in waveguide  $D_2$  is always vanishing because it couples to the lossy channel  $D_3$ . Next we concentrate our discussion in the nonreciprocal



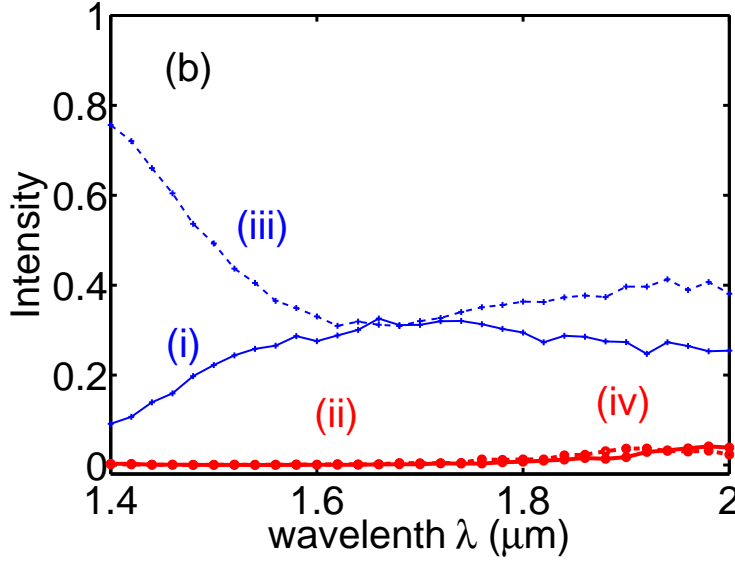


Fig. 4. Nonreciprocal transmission as a function of frequency of input light using structure as in Fig. 3 (a). Thin blue lines (i) and (iii) show the light trapped in waveguide  $D_1$ , thick red lines (ii) and (iv) show the light energy in  $D_2$ . Solid lines for light launching to  $D_2$ , dashed lines for light input into  $D_1$ .

window of interest. It can be clearly seen in Fig. 4, whatever waveguide the light is incident to, about 30% energy is trapped in  $D_1$  and comes out of port  $P_{R1}$ . The weak frequency-dependence of transmission comes from the change of eigenmode profiles and their couplings  $\kappa_{13}$  and  $\kappa_{23}$ , which are also dependent on the profiles of eigenmodes and wavelength [ref. to Eq. (5)]. The deviation in fabrication may result in a small difference between  $\Delta_{13}$  and  $\Delta_{23}$ . However the transmission change slightly if  $\Delta_{13} \approx \Delta_{23}$ .

#### 4. Conclusion

In conclusion, using a technique analogous to the coherent population trapping in quantum optics, we broke the symmetry of transverse light propagation in the photonic circuits of three coupled waveguides. Our proposed system is made only from linear, passive materials. Our simulations indicate the possibility of asymmetric transverse energy flow in an ultrabroadband window spanning over 200 nm in frequency. Although our proposed system has a relatively large insertion loss, it opens a door to the possibility of highly efficient optical nonreciprocity in a linear, passive medium.

#### 5. Acknowledgement

This research is supported by a grant from the King Abdulaziz City for Science and Technology (KACST). One of us (MSZ) is grateful for the NPRP grant 5-102-1-071 from the Qatar National Research Fund (QNRF). KX also gratefully acknowledge the hospitality at ARC Center for Engineered Quantum Systems and Department of Physics and Astronomy, Macquarie University.